Supporting information for

Chiroptical Activity in BINAP– and DIOP– stabilized Octa– and Undecagold Clusters

Natalia V. Karimova, Christine M. Aikens
Department of Chemistry, Kansas State University, Manhattan, KS 66506, USA
*cmaikens@ksu.edu, 1-785-532-0954, fax: 1-785-532-6666

Page **Contents**

Geometrical Structure of $[Au_{11}X_4Cl_2]^+$ and $[Au_8X_3(PH_3)_2]^{2+}$ (X = L1, L2)

$[Au_{11}X_4Cl_2]^+$ (X = L1, L2) clusters: chlorine atom positions. To identify the most stable isomers of $[Au_{11}X_4Cl_2]^+$ (X = L1, L2) clusters we need to find the preferred arrangement of the four L1 or L2 bridging ligands around the Au_{11} gold core and the position of the two chlorine atoms, each of which is attached to one gold atom. The geometrical structure of some undecagold clusters has previously been investigated experimentally[1-2] and theoretically.[3] Crystal structures were determined for undecagold clusters protected by achiral[2] and chiral[1] ligands: $[Au_{11}(PPh_3)_8Cl_2]^+$ and $[Au_{11}(DIOP)_4Cl_2]^+$. The obtained results showed that the structure of the Au_{11} fragment in both types of clusters (with mono– and bidentate ligands) is an incomplete icosahedral structure: a central gold atom (yellow color) is located between a pentagonal pyramid (6 gold atoms in dark purple color) and a rectangular gold ring (4 gold atoms in blue) (Figure S1). The distances between the central gold atom and the gold atoms of the shell are 2.639–2.700 Å for the cluster stabilized by PPh_3 ligands, and 2.641–2.695 Å in the case of chiral DIOP ligands. Average distances between gold atoms and phosphine groups are ~2.280 and 2.282 Å for $[Au_{11}(PPh_3)_8Cl_2]^+$ and $[Au_{11}(DIOP)_4Cl_2]^+$, correspondingly (Table S1). The position of the two chlorine atoms near the Au_{11} core is different for clusters protected by PPh_3 and DIOP ligands (Figure S1). For the monodentate phosphine system $[Au_{11}(PPh_3)_8Cl_2]^+$, the two chlorine atoms are attached to two opposite gold atoms on a 5-fold ring of the pentagonal pyramid base (denoted as the 5,5–position) (Figure S1b),[2] whereas in the case of $[Au_{11}(DIOP)_4Cl_2]^+$ one chlorine atom is attached to a gold atom on the pentagonal ring and the second one is connected to the opposite gold atom from the 4–fold ring (denoted as the 4,5–position), so that they are located on the same axis (Figure S1a).[1]

A previous theoretical investigation[3] of the geometrical structure was performed for $[Au_{11}(PH_3)_8Cl_2]^+$ and $[Au_{11}(L2)_4X_2]^+$ (where X = Cl, Br) using the Xα local density approximation (LDA) functional with a TZP frozen core basis set. For the cluster protected by monodentate ligands, the obtained theoretical results are very close to the experimental data for the $[Au_{11}(PPh_3)_8Cl_2]^+$ cluster: the geometrical structure of the gold core and the chlorine atoms positions are similar (5,5–position) for experiment and theory. For the simulation of $[Au_{11}(BINAP)_4X_2]^+$ clusters, only systems with chlorine atoms positions near opposite gold atoms on a 5-fold ring were reported (5,5–

position) because systems with the 4,5–position were found to be higher in energy. In order to determine the position of the chlorine atoms in the $[Au_{11}X_4Cl_2]^+$ (X = L1, L2) model clusters, all possible positions of the chlorine atoms are considered in this work.

Figure S1. (a), (b) Structures of the $Au_{11}Cl_2$ fragment of clusters $[Au_{11}(DIOP)_4Cl_2]^+$ and $[Au_{11}(PPh_3)_8Cl_2]^+$ from the corresponding x-ray crystal structures[1, 2]; (c) structure of the $Au_8(PH_3)_2$ fragment (with H substituted for Ph rings) from the crystal structure[1] of $[Au_8(BINAP)_3(PPh_3)_2]^{2+}$. Gold atoms – yellow, blue and dark purple; chlorine atom – green; phosphorous – light purple; hydrogen – white.

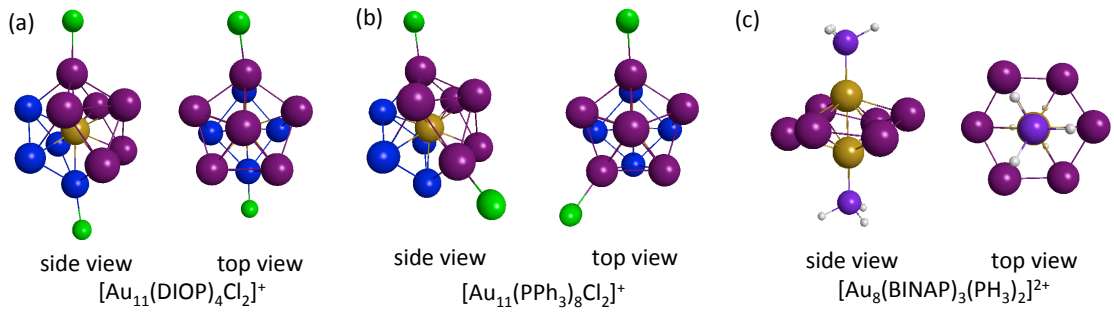

To identify preferable chlorine locations in the $[Au_{11}X_4Cl_2]^+$ (X = L1, L2) model clusters, all possible positions of the two Cl atoms were first considered for the undecagold cluster protected by simple phosphine ligands $[Au_{11}(PH_3)_8Cl_2]^+$. During the geometry optimization procedure, three main geometrical structures of $[Au_{11}(PH_3)_8Cl_2]^+$ were obtained with energy differences up to 1.6 kcal/mol in the gas phase (Figure 3). The results showed that the most stable isomer is $[Au_{11}(PH_3)_8Cl_2]^+$ (**1**) where the Cl atoms are attached in the 4,5–position, and the next most stable structure is $[Au_{11}(PH_3)_8Cl_2]^+$ (**2**) with the 5,5–position for chlorine atoms. The geometries of the undecagold cores in the $[Au_{11}(PH_3)_8Cl_2]^+$ structures (**1**) and (**2**) are similar to each other and to the crystal structure of $[Au_{11}(PPh_3)_8Cl_2]^+$ system. The least stable isomer (**3**) is obtained when one chlorine atom is attached to a gold atom of the pentagonal pyramid base and a second one to the top gold atom of this pyramid (denoted as the 5,5'–position). During the geometry optimization procedure for $[Au_{11}(PH_3)_8Cl_2]^+$ (**3**), the Au_{11} fragment was significantly deformed and exhibits a very different structure with respect to the experimental core. The energy difference between $[Au_{11}(PH_3)_8Cl_2]^+$ (**1**) and (**2**) is small (~1.0 kcal/mol in the gas phase) and the gold core fragments are similar these two isomers, so both chlorine atom positions could potentially be possible in real clusters with various ligands. Therefore, two types of chlorine atom positions (4,5– and 5,5–positions) are examined during geometry optimizations of the $[Au_{11}X_4Cl_2]^+$ (X = L1, L2) clusters.

$[Au_{11}X_4Cl_2]^+$ (X = L1, L2): ligand arrangement. In order to find the geometries of $[Au_{11}X_4Cl_2]^+$ (X = L1, L2) clusters, the eight achiral PH_3 groups in $[Au_{11}(PH_3)_8Cl_2]^+$ (**1**) and (**2**) clusters were substituted by four model bridging ligands L1 and L2 (Figure 3). The possible structures were limited by the bond lengths and angles in the bisphosphine ligands. The geometries of all considered isomers were optimized in the gas phase first, followed

by further optimization of the most energetically preferable in continuum solvent (using COSMO) as described below. All obtained isomers and their relative energies in the gas phase can be found in Figures S3 and S4. The most energetically stable gas phase isomers of $[Au_{11}X_4Cl_2]^+$ (X = L1, L2) are $[Au_{11}(L1)_4Cl_2]^+$ (**4**), $[Au_{11}(L2)_4Cl_2]^+$ (**5**), $[Au_{11}(L1)_4Cl_2]^+$ (**6**) and $[Au_{11}(L2)_4Cl_2]^+$ (**7**) (shown in Figure 4a**)**. In the gas phase, these clusters exhibit bond distances between the central gold atom and the shell atoms of the undecagold core in the range of 2.663–2.802 Å, chlorine atoms are attached to the Au atoms with bonds of 2.450–2.458 Å, and phosphine atoms are coordinated around the gold core with distances of 2.440–2.449 Å (Table S1). In complexes $[Au_{11}(L1)_4Cl_2]^+$ (**4**) and $[Au_{11}(L2)_4Cl_2]^+$ (**5**) the chlorine atoms are in the 4,5–position, whereas in $[Au_{11}(L1)_4Cl_2]^+$ (**6**) and $[Au_{11}(L2)_4Cl_2]^+$ (**7**) the Cl atoms are attached to the gold core in the 5,5–position. The theoretically calculated relative energies in the gas phase for these isomers show that structures with chlorine atoms in the 4,5–position are more preferable energetically in both cases (L1 and L2 ligands) (Figure 4a).

In the next step, the geometries of these most energetically stable (in the gas phase) isomers of $[Au_{11}X_4Cl_2]^+$ (X = L1, L2) were reoptimized including solvent effects. Comparison of the geometries for the $[Au_{11}(L1)_4Cl_2]^+$ (**4**), $[Au_{11}(L2)_4Cl_2]^+$ (**5**), $[Au_{11}(L1)_4Cl_2]^+$ (**6**) and $[Au_{11}(L2)_4Cl_2]^+$ (**7**) clusters in the gas and solution phases shows similarities and differences. For example, the shape of the Au_{11} gold core is very close in the gas phase and in chloroform. However, there are some differences in the bond lengths: distances between the central Au atom and the shell Au atoms (connected to the chlorine atoms) became shorter in chloroform by ~0.04 Å, whereas the distances between the central Au atom and shell Au atoms (connected to the phosphine ligands) and the Au–Cl bonds became longer by ~0.05 Å (Table S1). The structure of the Au_{11} core, the positions of the two chlorine atoms and the arrangement of the four bridging ligands in the experimental structure $[Au_{11}(DIOP)_4Cl_2]^+$ and theoretically predicted model structure $[Au_{11}(L1)_4Cl_2]^+$ (**4**) in chloroform are very similar. For example, overlay of the Au_{11} fragments of theoretical and experimental clusters showed that the shape of these undecagold cores is very close (Figure S2a). However, the Au–Au, Au–Cl and Au–P bonds are longer in the optimized cluster $[Au_{11}(L1)_4Cl_2]^+$ (**4**) with respect to the experimental structure $[Au_{11}(DIOP)_4Cl_2]^+$ by up to 0.091, 0.127 and 0.161 Å, correspondingly; these types of bond elongations are typical for the BP86 exchange-correlation functional used in the DFT optimizations.

Figure S2. Superposition of experimental and theoretical gold cores (in chloroform): (a) Au_{11} core and (b) Au_8 core. Color key: experiment – blue and theory – yellow.

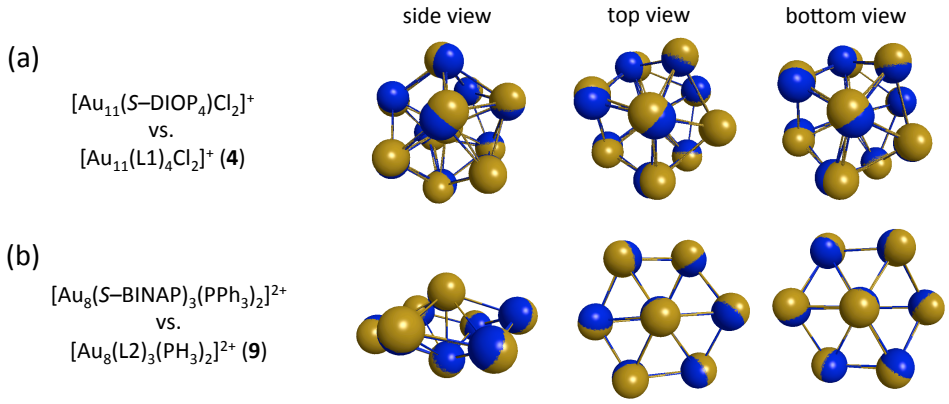

Theoretically calculated relative energies for gas phase structures of $[Au_{11}(L1)_4Cl_2]^+$ (**4**), $[Au_{11}(L2)_4Cl_2]^+$ (**5**), $[Au_{11}(L1)_4Cl_2]^+$ (**6**) and $[Au_{11}(L2)_4Cl_2]^+$ (**7**) clusters showed that structures with chlorine atoms in the 4,5–position are energetically more preferable for both L1 and L2 ligands (Figure 4a). However, solvent effects change this for systems protected by L2 ligands: the $[Au_{11}(L2)_4Cl_2]^+$ (**7**) cluster with the 5,5–chlorine atom position is more energetically stable by 0.18 kcal/mol with respect to the $[Au_{11}(L2)_4Cl_2]^+$ (**5**) cluster. Due to the small differences in the relative energies between the isomers, optical absorption and CD spectra were calculated for $[Au_{11}(L1)_4Cl_2]^+$ (**4**), $[Au_{11}(L2)_4Cl_2]^+$ (**5**), $[Au_{11}(L1)_4Cl_2]^+$ (**6**) and $[Au_{11}(L2)_4Cl_2]^+$ (**7**) clusters both in gas phase and in chloroform.

$[Au_8X_3(PH_3)_2]^{2+}$ (X = L1, L2). The x–ray crystal structure of $[Au_8(BINAP)_3(PPh_3)_2]^{2+}$ was determined by Tsukuda and co–workers.[1] Their results showed that the Au_8 gold core does not depart very much from C_{3v} symmetry: six Au atoms (dark purple) form a "chair–cyclohexane" structure with one gold atom added above and one below the ring (Figure 4c and S1c). The measured Au–Au bond distances in the crystal structure are typical for gold systems and are in the range of 2.523 to 3.109 Å (Table S2). Two achiral triphenylphosphine ligands are attached to the top gold atoms above and below the 6–fold ring with a distance of 2.303 Å and they create a central axis (Ph_3P–Au–Au–PPh_3) in the $[Au_8(BINAP)_3(PPh_3)_2]^{2+}$ cluster. Three BINAP ligands are bound to the octagold core through six equatorial surface atoms (atoms of the hexagonal ring) with an average distance of 2.305 Å (Table S2).

To simulate $[Au_8(BINAP)_3(PPh_3)_2]^{2+}$ and $[Au_8(DIOP)_3(PPh_3)_2]^{2+}$ clusters, the theoretical models $[Au_8X_3(PH_3)_2]^{2+}$ (X = L1, L2) were used. The DIOP and BINAP ligands were substituted by the L1 and L2 model ligands and PPh_3 groups were exchanged for simple PH_3. In theoretical clusters $[Au_8X_3(PH_3)_2]^{2+}$ (X = L1, L2), positions of the PH_3 groups and the model bridging ligands are similar to the known experimental structure $[Au_8(BINAP)_3(PPh_3)_2]^{2+}$: two monodentate phosphine ligands (PH_3) are coordinated on the top and the bottom of the gold core, and bridging ligands L1 and L2 are bound to the octagold core through gold atoms of the "chair–

cyclohexane" ring (dark purple atoms in Figure S1c). Therefore, model clusters $[Au_8(L1)_3(PH_3)_2]^{2+}$ (**8**) and $[Au_8(L2)_3(PH_3)_2]^{2+}$ (**9**) were considered (Figure S2b).

Comparison of the Au_8 fragment geometry of the experimental structure $[Au_8(BINAP)_3(PPh_3)_2]^{2+}$ and the theoretically predicted model structure $[Au_8(L2)_3(PH_3)_2]^{2+}$ (**9**) are very close (Figure S2b**,** Table S2). Gold–gold distances are longer in the theoretical structure by up to 0.16 Å with respect to experimental gold core in both gas phase and chloroform; again, this is typical of the BP86 functional employed in the optimizations. Experimental DIOP and BINAP ligands have shorter Au-P bonds than the Au-P bonds present in optimized clusters containing the L1 and L2 model ligands, with differences of 0.127–0.193 Å. Full geometry optimization was performed only for the $[Au_8(L2)_3(PH_3)_2]^{2+}$ (**9**) structure because dramatic changes happened in the gold core during optimization of $[Au_8(L1)_3(PH_3)_2]^{2+}$. To obtain the $[Au_8(L1)_3(PH_3)_2]^{2+}$ (**8**) structure shown in Figure 4b, the Au_8 fragment was frozen during optimization (i.e. the gold core geometry was used from the optimized $[Au_8(L2)_3(PH_3)_2]^{2+}$ (**9**) cluster), and only optimization of the L1 shell was performed.

Figure S3. The most stable isomers of the $Au_{11}(L1)_4Cl_2^+$ cluster at the BP86/DZ.fc level of theory in the gas phase. Hydrogen atoms are not shown for clarity.

4,5–position of Cl atoms

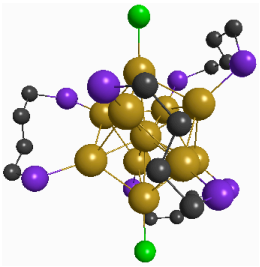

$Au_{11}(L1)_4Cl_2^+$ (**4**)
0.00 kcal/mol

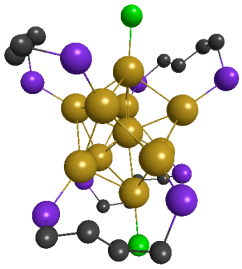

$Au_{11}(L1)_4Cl_2^+$ (**4–b**)
0.71 kcal/mol

5,5–position of Cl atoms

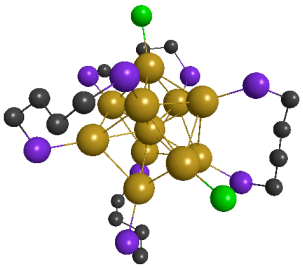

$Au_{11}(L1)_4Cl_2^+$ (**6**)
0.78 kcal/mol

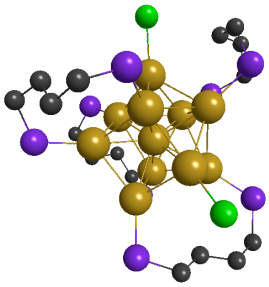

$Au_{11}(L1)_4Cl_2^+$ (**6–b**)
3.22 kcal/mol

Figure S4. The most stable isomers of the $Au_{11}(L2)_4Cl_2^+$ cluster at the BP86/DZ.fc level of theory in the gas phase. Hydrogen atoms are not shown for clarity.

4,5–position of Cl atoms

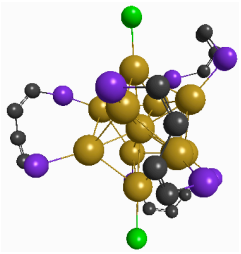

$Au_{11}(L2)_4Cl_2^+$ (**5**)
0.00 kcal/mol

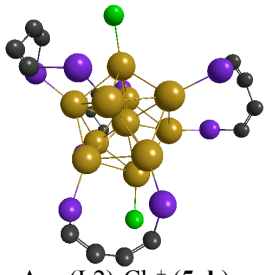

$Au_{11}(L2)_4Cl_2^+$ (**5–b**)
0.26 kcal/mol

5,5–position of Cl atoms

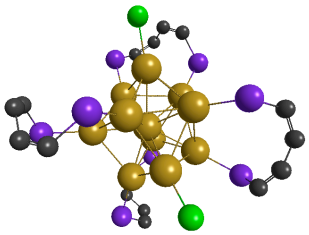

$Au_{11}(L2)_4Cl_2^+$ (**7**)
0.46 kcal/mol

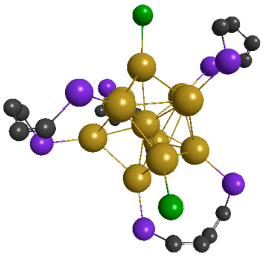

$Au_{11}(L2)_4Cl_2^+$ (**7–b**)
0.90 kcal/mol

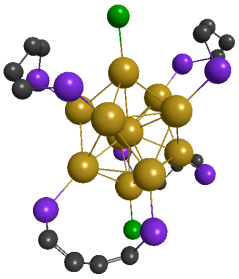

$Au_{11}(L2)_4Cl_2^+$ (**5–c**)
2.51 kcal/mol

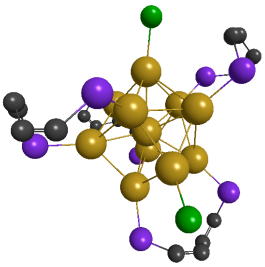

$Au_{11}(L2)_4Cl_2^+$ (**7–c**)
1.00 kcal/mol

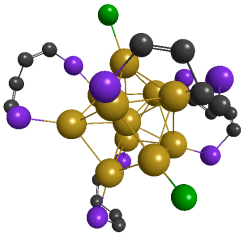

$Au_{11}(L2)_4Cl_2^+$ (**7–d**)
2.19 kcal/mol

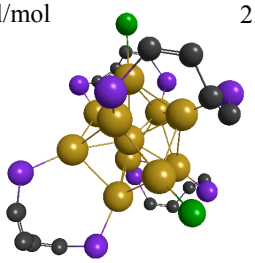

$Au_{11}(L2)_4Cl_2^+$ (**7–b**)
2.48 kcal/mol

Figure S5. Gold atom positions in the isolated Au_{11}^{3+} gold core.

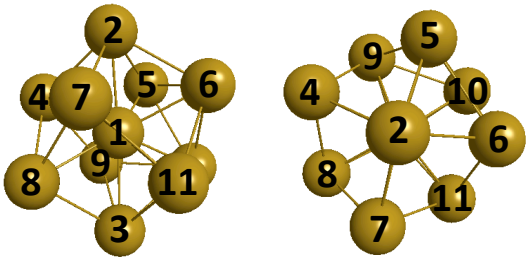

Table S1. Geometrical parameters for experimental crystal structures $Au_{11}(DIOP)_4Cl_2^+$ and $Au_{11}(PPh_3)_8Cl_2^+$ and theoretical structures $Au_{11}X_4Cl_2^+$ where X = L1, L2.

Parameter	Experiment [1, 2]		Theory (BP86/DZ.fc)							
			Gas				COSMO			
	$Au_{11}(DIOP)_4Cl_2^+$	$Au_{11}(PPh_3)_8Cl_2^+$	Complex (4)	Complex (6)	Complex (5)	Complex (7)	Complex (4)	Complex (6)	Complex (5)	Complex (7)
Au1Au2	2.689	2.713	2.782	2.791	2.763	2.802	2.724	2.768	2.729	2.772
Au1Au3	2.689	2.689	2.773	2.688	2.765	2.682	2.767	2.696	2.740	2.693
Au1Au4	2.641	2.639	2.694	2.701	2.696	2.712	2.732	2.693	2.713	2.703
Au1Au5	2.695	2.695	2.727	2.73	2.732	2.734	2.736	2.743	2.742	2.743
Au1Au6	2.685	2.701	2.728	2.752	2.735	2.746	2.732	2.742	2.745	2.748
Au1Au7	2.657	2.728	2.676	2.694	2.682	2.695	2.680	2.700	2.691	2.705
Au1Au8	2.657	2.677	2.675	2.663	2.679	2.667	2.705	2.679	2.695	2.688
Au1Au9	2.685	2.644	2.731	2.709	2.738	2.701	2.732	2.731	2.750	2.717
Au1Au10	2.695	2.688	2.725	2.73	2.731	2.733	2.732	2.734	2.743	2.746
Au1Au11	2.642	2.700	2.699	2.789	2.702	2.776	2.697	2.772	2.709	2.754
Au2Cl	2.378	2.355	2.454	2.450	2.451	2.458	2.504	2.505	2.496	2.500
Au3Cl	2.378	_	2.454	_	2.452	_	2.505	_	2.498	_
Au11Cl	_	2.356	_	2.452	_	2.449	_	2.509	_	2.501
Au…P	~2.282	~2.28	~2.443	~2.440	~2.449	~2.447	~2.443	~2.441	~2.449	~2.445

Figure S6. Gold atom positions in $Au_8(PH_3)_2$ fragment.

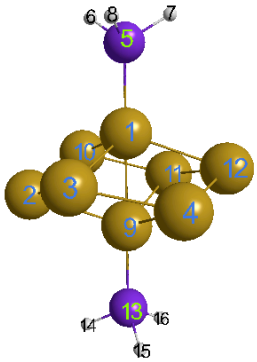

Table S2. Geometrical parameters for experimental crystal structures $[Au_8(BINAP)_3(PPh_3)_2]^{2+}$ and theoretical structures $Au_8X_3(PH_3)_2^{2+}$ where X = L1, L2.

	Experiment [2]	Theory (BP86/DZ.fc) gas phase	
	$[Au_8(BINAP)_3(PPh_3)_2]^{2+}$	(**8**)	(**9**)
Au (1)–Au(9)	2.523	2.593	2.593
Au (1)–Au(2)	3.103	3.182	3.182
Au (1)–Au(3)	2.803	2.867	2.867
Au (1)–Au(4)	3.022	3.124	3.124
Au (1)–Au(10)	2.856	2.846	2.846
Au (1)–Au(11)	3.109	3.127	3.127
Au (1)–Au(12)	2.825	2.863	2.863
Au (9)–Au(2)	2.786	2.846	2.846
Au (9)–Au(3)	3.109	3.127	3.127
Au (9)–Au(4)	2.856	2.863	2.863
Au (9)–Au(10)	3.022	3.182	3.182
Au (9)–Au(11)	2.803	2.867	2.867
Au (9)–Au(12)	3.103	3.124	3.124
Au(1)–P(5)	2.303	2.430	2.433
Au(9)–P(13)	2.303	2.430	2.433
~<Au–(P^P)>	2.305	2.498	2.487

Figure S7. UV–vis and CD spectra of a) $[Au_{11}(L1)_4Cl_2]^+$ (4), b) $[Au_{11}(L1)_4Cl_2]^+$ (6), c) $[Au_{11}(L2)_4Cl_2]^+$ (5), d) $[Au_{11}(L2)_4Cl_2]^+$ (7), e) $[Au_8(L1)_3(PH_3)_2]^{2+}$ (8), and f) $[Au_8(L2)_3(PH_3)_2]^{2+}$ (9) structures. Method: LB94/DZ.fc (gas phase).

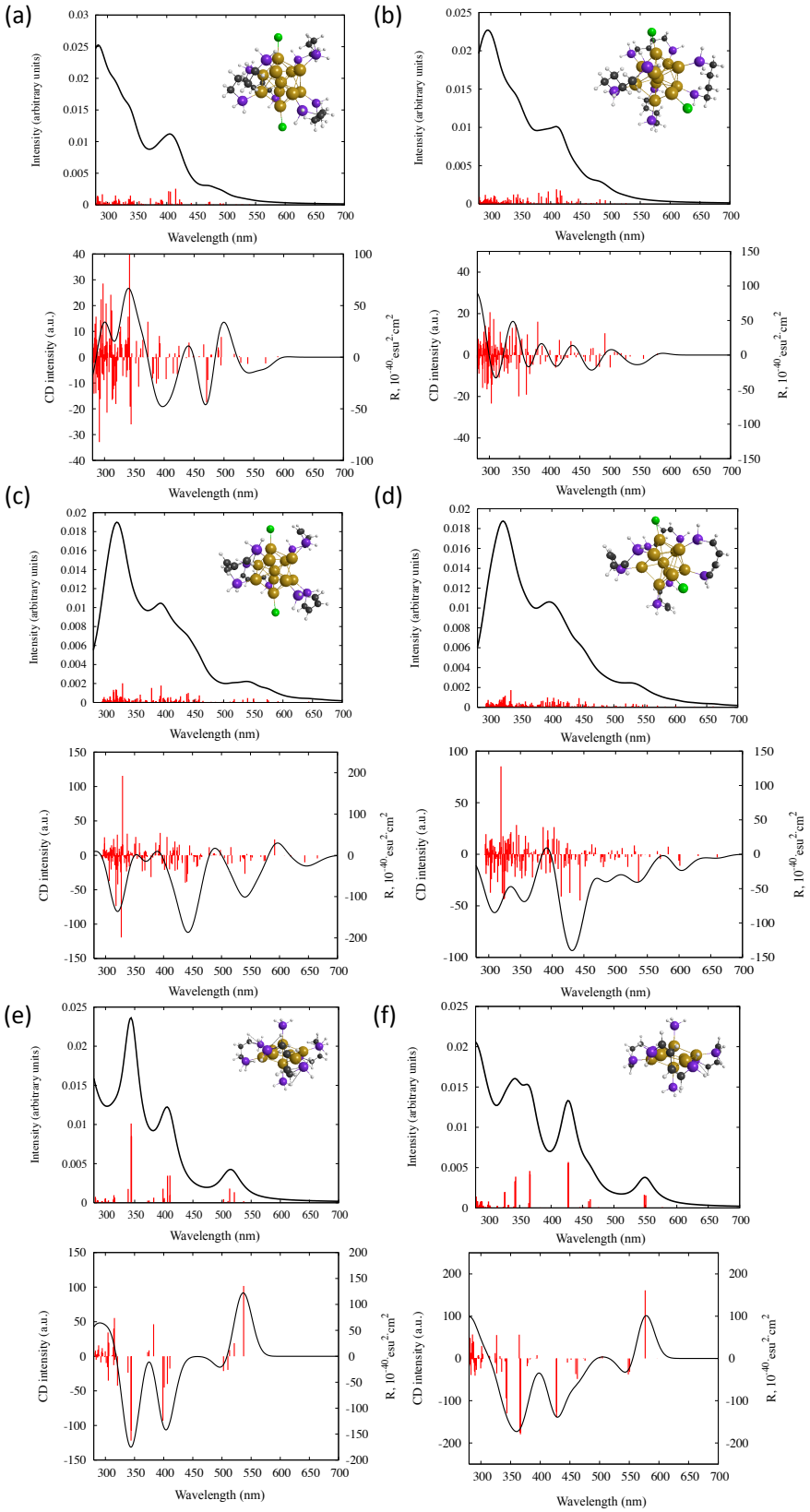

Table S3. Optical absorption and CD data for $[Au_{11}(L1)_4Cl_2]^+$ (4): peak positions, excited state wavelength, oscillator strengths (*f*), rotatory strengths (*R*, 10^{-40} esu^2cm^2), and orbitals involved in electronic transitions. Method LB94/DZ.fc (in chloroform).

				Excited state			f	R				Transition dipole moment				
ABS		CD							Electron transitions		Weight				Orbitals involved	
#	Peak, nm	#	Peak, nm	no.	E/eV	E/nm			From	To		x	y	z	from	to
–	–	1	533	1	2.301	539	0.0005	-1.07	187a	188a	0.9653	0.5731	0.3044	0.2101	HOMO	LUMO
				2	2.409	515	0.0006	-0.66	187a	189a	0.3932	0.0657	-1.947	0.5001	HOMO	LUMO+1
									186a	188a	0.3611	0.7227	1.0109	-1.5059	HOMO–1	LUMO
									185a	188a	0.1633	-1.273	0.4826	0.0162	HOMO–2	LUMO
				3	2.481	500	0.0056	0.39	186a	189a	0.5707	0.2371	0.6848	0.854	HOMO–1	LUMO+1
									185a	189a	0.1813	0.0564	-0.2694	-1.1543	HOMO–2	LUMO+1
									186a	188a	0.0941	-0.3635	-0.5084	0.7574	HOMO–1	LUMO
									185a	188a	0.0884	-0.9228	0.3499	0.0117	HOMO–2	LUMO
I	459	2	481	4	2.512	494	0.0257	1.70	186a	190a	0.3188	-0.7829	1.1654	0.3271	HOMO–1	LUMO+2
									187a	189a	0.2365	0.0499	-1.4786	0.3798	HOMO	LUMO+1
									185a	188a	0.213	1.4238	-0.5398	-0.0181	HOMO–2	LUMO
									185a	189a	0.1298	0.0475	-0.2265	-0.9707	HOMO–2	LUMO+1
				5	2.541	488	0.0128	-6.21	185a	190a	0.2663	-0.2109	-0.5677	0.3158	HOMO–2	LUMO+2
									186a	189a	0.2435	0.153	0.4421	0.5513	HOMO–1	LUMO+1
									187a	190a	0.1472	-0.6416	-0.4559	-1.0521	HOMO	LUMO+2
									186a	188a	0.1342	0.4291	0.6002	-0.894	HOMO–1	LUMO
									185a	188a	0.1025	0.9822	-0.3724	-0.0125	HOMO–2	LUMO
				7	2.628	472	0.0732	-42.48	187a	191a	0.2385	0.2319	-0.1938	-0.03	HOMO	LUMO+3
									185a	188a	0.1922	1.3224	-0.5014	-0.0168	HOMO–2	LUMO
									186a	191a	0.1785	-1.2756	0.2765	-0.2712	HOMO–1	LUMO+3
									187a	190a	0.1659	0.6698	0.4759	1.0984	HOMO	LUMO+2
				9	2.650	468	0.0726	35.30	185a	190a	0.4586	-0.2711	-0.7295	0.4057	HOMO–2	LUMO+2
									186a	188a	0.1747	-0.4793	-0.6704	0.9987	HOMO–1	LUMO
									185a	191a	0.1274	0.3079	0.6769	-0.7293	HOMO–2	LUMO+3
		3	453	10	2.703	459	0.1498	26.89	185a	189a	0.2579	-0.0645	0.3079	1.3192	HOMO–2	LUMO+1
									186a	190a	0.1702	-0.5515	0.821	0.2305	HOMO–1	LUMO+2
									187a	190a	0.154	0.6363	0.4521	1.0435	HOMO	LUMO+2
									187a	192a	0.0965	0.8352	-0.0967	-0.4695	HOMO	LUMO+4
II	412	4	423	13	2.943	421	0.6122	-47.74	185a	191a	0.4381	0.5419	1.1913	-1.2834	HOMO–2	LUMO+3
									186a	191a	0.2153	-1.324	0.2869	-0.2814	HOMO–1	LUMO+3
				14	3.006	412	0.6170	-5.33	187a	192a	0.27	1.3245	-0.1534	-0.7446	HOMO	LUMO+4
									186a	192a	0.2207	-0.2078	-0.8424	-0.4863	HOMO–1	LUMO+4
									186a	191a	0.0959	0.8745	-0.1895	0.1859	HOMO–1	LUMO+3
		5	385	15	3.064	405	0.6598	23.95	185a	192a	0.3222	0.6879	0.9196	0.4351	HOMO–2	LUMO+4
									186a	191a	0.1329	1.0195	-0.2209	0.2167	HOMO–1	LUMO+3

									187a	192a	0.122	0.8819	-0.1021	-0.4957	HOMO	LUMO+4
III	351s	6	349	25	3.536	351	0.1609	7.94	181a	189a	0.2849	0.3746	-0.486	0.4641	HOMO–6	LUMO+1
									181a	188a	0.2152	-0.7274	0.0008	0.4457	HOMO–6	LUMO
				26	3.557	349	0.0674	0.81	187a	193a	0.5044	-0.0338	0.4077	-0.1122	HOMO	LUMO+5
									181a	189a	0.1405	0.2623	-0.3403	0.325	HOMO–6	LUMO+1
									181a	188a	0.1082	0.5142	-0.0005	-0.3151	HOMO–6	LUMO
				28	3.576	347	0.0708	5.46	181a	189a	0.3867	-0.4339	0.563	-0.5377	HOMO–6	LUMO+1

Table S4. Optical absorption and CD data for $[Au_{11}(L1)_4Cl_2]^+$ (6): peak positions, excited state wavelength, oscillator strengths (*f*), rotatory strengths (*R*, 10^{-40} esu^{2}cm^2), and orbitals involved in electronic transitions. Method LB94/DZ.fc (in chloroform).

ABS		CD		Excited state			f	R	Electron transitions		Weight	Transition dipole moment			Orbitals involved	
#	Peak, nm	#	Peak, nm	no.	E/eV	E/nm			From	To		x	y	z	from	to
I	480s	1	493	4	2.52	492	0.027	-29.92	187a	189a	0.3079	-0.335	0.293	-1.713	HOMO	LUMO+1
									187a	190a	0.284	0.642	1.538	0.334	HOMO	LUMO+2
									185a	188a	0.1504	-1.163	-0.495	0.556	HOMO–2	LUMO
				6	2.58	480	0.048	-4.00	187a	191a	0.2343	0.612	-0.065	-0.245	HOMO	LUMO+3
									187a	189a	0.2029	0.269	-0.235	1.374	HOMO	LUMO+1
									187a	190a	0.1884	0.517	1.238	0.269	HOMO	LUMO+2
									186a	191a	0.1263	-0.896	-0.632	-0.203	HOMO–1	LUMO+3
				7	2.63	471	0.029	-28.41	185a	190a	0.2383	-0.130	0.685	0.449	HOMO–2	LUMO+2
									185a	188a	0.2146	1.361	0.579	-0.651	HOMO–2	LUMO
									186a	191a	0.1566	-0.988	-0.697	-0.224	HOMO–1	LUMO+3
									186a	190a	0.0997	0.828	-0.379	0.061	HOMO–1	LUMO+2
									187a	192a	0.0776	-0.652	0.230	0.233	HOMO	LUMO+4
		2	460	9	2.66	465	0.039	38.17	186a	190a	0.2405	-1.278	0.585	-0.094	HOMO–1	LUMO+2
									187a	191a	0.1867	0.538	-0.057	-0.215	HOMO	LUMO+3
									185a	190a	0.1404	0.099	-0.523	-0.343	HOMO–2	LUMO+2
									185a	188a	0.1192	1.008	0.429	-0.482	HOMO–2	LUMO
									186a	188a	0.1136	-0.228	0.503	-0.592	HOMO–1	LUMO
				10	2.70	460	0.012	29.51	187a	192a	0.4882	-1.617	0.570	0.578	HOMO	LUMO+4
									185a	190a	0.19	0.115	-0.605	-0.396	HOMO–2	LUMO+2
									186a	191a	0.1402	0.924	0.651	0.209	HOMO–1	LUMO+3
									185a	189a	0.0593	0.078	-0.601	-0.186	HOMO–2	LUMO+1
									186a	190a	0.0376	0.502	-0.230	0.037	HOMO–1	LUMO+2
				11	2.73	454	0.036	29.75	186a	192a	0.517	-0.189	0.142	1.620	HOMO–1	LUMO+4
									185a	191a	0.2284	-0.282	0.332	-1.055	HOMO–2	LUMO+3
									187a	192a	0.0831	0.663	-0.234	-0.237	HOMO	LUMO+4
									185a	192a	0.0309	-0.252	0.202	-0.219	HOMO–2	LUMO+4
II	418	3	430	12	2.78	446	0.070	-4.28	185a	192a	0.4517	0.955	-0.768	0.829	HOMO–2	LUMO+4
									185a	191a	0.327	-0.335	0.394	-1.251	HOMO–2	LUMO+3
				13	2.91	426	0.669	-160.91	186a	191a	0.2888	1.276	0.900	0.289	HOMO–1	LUMO+3

									187a	190a	0.1868	0.485	1.161	0.252	HOMO	LUMO+2
									185a	189a	0.1436	-0.117	0.900	0.278	HOMO–2	LUMO+1
				14	2.96	420	0.685	33.05	187a	192a	0.2078	-1.008	0.355	0.360	HOMO	LUMO+4
		4	400						185a	188a	0.1816	-1.181	-0.503	0.565	HOMO–2	LUMO
				15	3.01	412	0.684	76.13	185a	192a	0.3992	0.863	-0.694	0.750	HOMO–2	LUMO+4
									185a	191a	0.2019	0.253	-0.297	0.945	HOMO–2	LUMO+3
									186a	190a	0.0687	0.643	-0.294	0.047	HOMO–1	LUMO+2
III	348s	5	345	21	3.45	359	0.024	26.57	183a	189a	0.4815	0.207	0.353	0.216	HOMO–4	LUMO+1
									183a	188a	0.2878	0.585	0.106	-0.054	HOMO–4	LUMO
				27	3.55	349	0.024	-19.24	182a	190a	0.5123	0.092	0.202	0.292	HOMO–5	LUMO+2
									183a	190a	0.1496	-0.013	0.280	0.065	HOMO–4	LUMO+2
									181a	190a	0.1262	0.032	0.055	-0.075	HOMO–6	LUMO+2
									180a	188a	0.0589	-0.402	-0.181	0.176	HOMO–7	LUMO
				28	3.56	348	0.151	10.28	180a	188a	0.4297	-1.084	-0.487	0.476	HOMO–7	LUMO
				31	3.62	343	0.029	11.53	187a	193a	0.5987	0.112	0.029	-0.236	HOMO	LUMO+5
									186a	193a	0.207	0.292	0.212	0.105	HOMO–1	LUMO+5
				33	3.63	341	0.028	3.12	186a	193a	0.3973	-0.404	-0.294	-0.145	HOMO–1	LUMO+5
									180a	190a	0.1597	0.325	-0.580	0.264	HOMO–7	LUMO+2
				35	3.65	340	0.075	7.53	180a	190a	0.5406	-0.597	1.064	-0.485	HOMO–7	LUMO+2
		6	316	42	3.72	333	0.070	-31.19	187a	194a	0.4787	-0.690	0.750	0.543	HOMO	LUMO+6
				44	3.75	331	0.100	-42.60	186a	194a	0.3245	-0.622	0.315	-0.158	HOMO–1	LUMO+6
				50	3.82	325	0.070	-25.40	178a	188a	0.6079	0.399	0.047	-0.213	HOMO–9	LUMO
									186a	195a	0.1529	0.318	0.275	0.143	HOMO–1	LUMO+7
				66	4.02	309	0.069	-7.88	186a	197a	0.5099	0.942	0.343	0.689	HOMO–1	LUMO+9
				53	3.86	321	0.088	77.11	178a	189a	0.3334	0.143	-0.784	-0.117	HOMO–9	LUMO+1
				61	3.96	313	0.113	-2.03	176a	189a	0.2017	0.338	-0.060	-0.021	HOMO–11	LUMO+1
									187a	196a	0.1258	0.170	-0.183	0.003	HOMO	LUMO+8

Table S5. Optical absorption and CD data for $[Au_{11}(L2)_4Cl_2]^+$ (5): peak positions, excited state wavelength, oscillator strengths (f), rotatory strengths (R, 10^{-40} esu^2cm^2), and orbitals involved in electronic transitions. Method: LB94/DZ.fc (solvent = chloroform).

ABS		CD		Excited state			f	R	Electron transitions		Weight	Transition dipole moment			Orbitals involved	
#	Peak, nm	#	Peak, nm	no.	E/eV	E/nm			From	To		x	y	z	from	to
I	552s	1	568	1	2.186	567	0.013	-20.63	178a	180a	0.5159	0.4155	-0.4116	-1.1643	HOMO-1	LUMO
		2	533						179a	180a	0.4601	-0.8227	-0.733	1.2035	HOMO	LUMO
				2	2.245	552	0.032	6.59	179a	180a	0.4266	0.7818	0.6965	-1.1437	HOMO	LUMO
									178a	180a	0.4132	0.3669	-0.3636	-1.0283	HOMO-1	LUMO
				3	2.318	535	0.013	-16.86	179a	181a	0.6331	-0.8906	2.2768	-0.2345	HOMO	LUMO+1
									179a	182a	0.2558	-0.2228	-0.9775	-0.0752	HOMO	LUMO+2
II	497s	3	495	4	2.339	530	0.009	-4.59	178a	181a	0.415	1.5902	0.3693	1.356	HOMO-1	LUMO+1

									178a	182a	0.2765	-0.1607	-1.3458	-0.6466	HOMO-1	LUMO+2
									179a	182a	0.1246	0.1548	0.6791	0.0522	HOMO	LUMO+2
									177a	180a	0.1046	-0.7499	0.3606	-0.6776	HOMO-2	LUMO
				5	2.396	518	0.058	124.78	179a	182a	0.3532	0.2574	1.1297	0.0869	HOMO	LUMO+2
									178a	181a	0.3033	-1.3433	-0.312	-1.1454	HOMO-1	LUMO+1
									179a	181a	0.1217	-0.3841	0.9819	-0.1011	HOMO	LUMO+1
				7	2.468	502	0.081	-124.55	177a	181a	0.3106	0.1551	0.9654	0.3121	HOMO-2	LUMO+1
									178a	182a	0.2932	-0.1611	-1.3492	-0.6482	HOMO-1	LUMO+2
				8	2.486	499	0.065	-168.33	178a	183a	0.7842	1.5418	0.7959	-1.2145	HOMO-1	LUMO+3
				9	2.494	497	0.139	-121.40	177a	180a	0.6235	1.7733	-0.8526	1.6024	HOMO-2	LUMO
				10	2.549	486	0.030	-53.09	177a	181a	0.4048	-0.1742	-1.0846	-0.3506	HOMO-2	LUMO+1
									178a	184a	0.2712	-0.1923	0.8188	-0.1469	HOMO-1	LUMO+4
									179a	184a	0.213	0.5442	0.0637	0.6283	HOMO	LUMO+4
				11	2.566	483	0.128	-106.24	177a	183a	0.2681	0.237	1.1663	0.3719	HOMO-2	LUMO+3
									179a	184a	0.2079	-0.5358	-0.0627	-0.6186	HOMO	LUMO+4
III	452	4	440	12	2.583	480	0.017	34.76	178a	184a	0.3822	0.2268	-0.9657	0.1732	HOMO-1	LUMO+4
									177a	182a	0.2906	0.4858	0.358	-1.4033	HOMO-2	LUMO+2
				13	2.669	465	0.076	-27.95	179a	185a	0.7844	1.4191	-0.5082	-0.5923	HOMO	LUMO+5
				14	2.695	460	0.213	36.16	177a	182a	0.377	-0.5418	-0.3993	1.5649	HOMO-2	LUMO+2
				15	2.704	459	0.093	80.38	178a	185a	0.6273	-0.7704	-0.3341	0.0538	HOMO-1	LUMO+5
				16	2.718	456	0.184	71.64	177a	183a	0.3562	0.2654	1.3064	0.4166	HOMO-2	LUMO+3
				17	2.747	451	0.235	-133.59	177a	183a	0.1435	-0.1676	-0.8248	-0.263	HOMO-2	LUMO+3
				18	2.786	445	0.067	24.19	177a	184a	0.2182	-0.9692	-0.0226	0.5943	HOMO-2	LUMO+4
				19	2.799	443	0.225	-166.90	177a	184a	0.4363	1.3672	0.0319	-0.8384	HOMO-2	LUMO+4
IV	420	5	405	22	2.951	420	0.251	-40.99	179a	187a	0.2689	-1.2228	0.1701	-0.0136	HOMO	LUMO+7
									178a	187a	0.2322	-0.7453	0.1719	-0.0068	HOMO-1	LUMO+7
				24	3.061	405	0.098	-8.93	179a	188a	0.7017	-0.4014	0.8452	0.3779	HOMO	LUMO+8
				28	3.107	399	0.182	13.50	178a	188a	0.4003	-0.8855	-0.4052	0.0144	HOMO-1	LUMO+8
V	378s	6	373	30	3.182	390	0.041	-38.95	178a	189a	0.6961	-0.1459	-0.6816	0.5387	HOMO-1	LUMO+9
				40	3.282	378	0.164	165.92	172a	180a	0.5029	0.4653	0.2384	-0.8624	HOMO-7	LUMO
				45	3.326	373	0.015	37.39	179a	192a	0.6214	-0.1173	-0.1772	-0.1999	HOMO	LUMO+12
				50	3.371	368	0.056	-17.29	178a	192a	0.2484	0.0089	0.3399	-0.4129	HOMO-1	LUMO+12
									173a	182a	0.2251	-0.4112	0.1304	-0.0881	HOMO-6	LUMO+2
				51	3.376	367	0.125	-76.41	173a	182a	0.3369	0.5027	-0.1594	0.1077	HOMO-6	LUMO+2
				52	3.386	366	0.075	2.60	178a	192a	0.4036	0.0113	0.4324	-0.5251	HOMO-1	LUMO+12
				56	3.434	361	0.110	-43.62	177a	190a	0.3662	0.104	-0.0464	-0.4279	HOMO-2	LUMO+10
									172a	182a	0.3489	-0.8065	0.3006	-0.62	HOMO-7	LUMO+2
				59	3.450	359	0.089	106.08	177a	190a	0.4159	-0.1106	0.0493	0.455	HOMO-2	LUMO+10
									172a	182a	0.2289	-0.6517	0.2429	-0.5011	HOMO-7	LUMO+2
				60	3.472	357	0.036	30.59	172a	183a	0.8449	0.0095	0.6093	0.1498	HOMO-7	LUMO+3
				61	3.477	357	0.028	43.29	171a	181a	0.9144	-0.1753	0.1734	-0.589	HOMO-8	LUMO+1
				62	3.485	356	0.007	-42.34	170a	180a	0.9256	0.0221	0.0662	-0.1597	HOMO-9	LUMO

Table S6. Optical absorption and CD data for $[Au_{11}(L2)_4Cl_2]^+$ (7): peak positions, excited state wavelength, oscillator strengths (*f*), rotatory strengths (*R*, 10^{-40} esu^2cm^2), and orbitals involved in electronic transitions. Method LB94/DZ.fc (in chloroform).

				Excited state			f	R				Transition dipole moment				
ABS		CD							Electron transitions		Weight				Orbitals involved	
#	nm	#	nm	no.	E/eV	E/nm			From	To		x	y	z	from	to
I	558s	1	540	1	2.22	558	0.026	1.80	179a	180a	0.738	-2.244	-0.168	-0.852	HOMO	LUMO
									179a	181a	0.1387	0.474	-0.561	-0.200	HOMO	LUMO+1
				3	2.29	540	0.019	-15.20	179a	181a	0.6626	1.021	-1.206	-0.431	HOMO	LUMO+1
									179a	180a	0.0916	0.778	0.058	0.296	HOMO	LUMO
				4	2.35	527	0.021	-0.27	179a	182a	0.5617	0.630	0.614	1.331	HOMO	LUMO+2
									178a	182a	0.1535	0.170	-0.462	-0.908	HOMO–1	LUMO+2
									177a	181a	0.0937	-0.200	-0.395	-0.262	HOMO–2	LUMO+1
									179a	180a	0.0757	0.698	0.052	0.265	HOMO	LUMO
									177a	180a	0.0263	-0.066	-0.092	0.573	HOMO–2	LUMO
II	499s	2	490	8	2.48	499	0.132	-84.57	177a	180a	0.2601	0.200	0.280	-1.753	HOMO–2	LUMO
									179a	184a	0.2358	0.275	-0.308	0.560	HOMO	LUMO+4
									178a	181a	0.1705	0.265	1.469	-0.548	HOMO–1	LUMO+1
				9	2.52	491	0.057	-13.74	179a	184a	0.4798	0.389	-0.435	0.792	HOMO	LUMO+4
									178a	181a	0.1254	-0.225	-1.250	0.466	HOMO–1	LUMO+1
									177a	182a	0.0988	-0.747	0.516	-0.211	HOMO–2	LUMO+2
				10	2.54	488	0.101	-65.23	178a	184a	0.2412	-0.024	-0.613	-0.718	HOMO–1	LUMO+4
									178a	182a	0.2013	-0.187	0.509	1.001	HOMO–1	LUMO+2
									177a	181a	0.1326	0.229	0.452	0.300	HOMO–2	LUMO+1
									177a	180a	0.0997	-0.123	-0.172	1.073	HOMO–2	LUMO
				11	2.56	485	0.050	-53.59	178a	183a	0.5632	2.138	-0.056	0.211	HOMO–1	LUMO+3
									177a	182a	0.2985	-1.291	0.891	-0.365	HOMO–2	LUMO+2
				12	2.60	477	0.043	-48.50	178a	184a	0.4578	0.032	0.836	0.979	HOMO–1	LUMO+4
									177a	183a	0.3678	0.171	-0.984	-0.312	HOMO–2	LUMO+3
III	457	3	450	13	2.63	472	0.081	41.85	179a	185a	0.367	-1.143	-0.285	0.917	HOMO	LUMO+5
									177a	184a	0.217	0.963	0.556	0.146	HOMO–2	LUMO+4
									177a	183a	0.1456	0.107	-0.615	-0.195	HOMO–2	LUMO+3
									177a	182a	0.0957	-0.721	0.498	-0.204	HOMO–2	LUMO+2
									178a	183a	0.0688	-0.737	0.019	-0.073	HOMO–1	LUMO+3
				14	2.67	464	0.143	44.87	177a	183a	0.2147	-0.129	0.741	0.235	HOMO–2	LUMO+3
									179a	185a	0.1244	-0.660	-0.164	0.530	HOMO	LUMO+5
				15	2.69	460	0.410	-147.54	177a	182a	0.2482	-1.147	0.792	-0.324	HOMO–2	LUMO+2
									179a	185a	0.1426	0.704	0.175	-0.565	HOMO	LUMO+5
									178a	183a	0.0916	-0.840	0.022	-0.083	HOMO–1	LUMO+3
									179a	184a	0.0841	-0.158	0.176	-0.321	HOMO	LUMO+4

									178a	181a	0.0703	0.163	0.906	-0.338	HOMO–1	LUMO+1
				16	2.73	455	0.053	29.64	178a	185a	0.5871	-0.311	0.019	0.152	HOMO–1	LUMO+5
									179a	186a	0.1537	0.358	-0.144	-0.457	HOMO	LUMO+6
									178a	184a	0.0522	0.011	0.276	0.323	HOMO–1	LUMO+4
									178a	183a	0.0324	-0.497	0.013	-0.049	HOMO–1	LUMO+3
									179a	185a	0.0282	-0.311	-0.077	0.250	HOMO	LUMO+5
				17	2.75	452	0.278	-69.75	177a	184a	0.5297	1.472	0.850	0.223	HOMO–2	LUMO+4
				18	2.79	444	0.103	-96.33	179a	186a	0.5521	0.670	-0.270	-0.856	HOMO	LUMO+6
									177a	185a	0.1408	-0.246	-0.099	0.251	HOMO–2	LUMO+5
									179a	185a	0.0712	0.488	0.122	-0.392	HOMO	LUMO+5
				19	2.82	439	0.066	-46.84	177a	185a	0.603	0.506	0.204	-0.517	HOMO–2	LUMO+5
									179a	187a	0.1044	-0.196	-0.319	-0.055	HOMO	LUMO+7
				20	2.87	432	0.176	-6.97	179a	187a	0.6168	0.472	0.767	0.133	HOMO	LUMO+7
IV	413s	4	408	21	2.88	430	0.064	-19.01	178a	186a	0.774	-0.170	-0.295	0.419	HOMO–1	LUMO+6
				22	2.94	422	0.116	28.76	178a	187a	0.64	0.827	0.133	-0.576	HOMO–1	LUMO+7
				24	3.01	413	0.125	6.10	179a	188a	0.4313	-1.117	0.391	0.279	HOMO	LUMO+8
				26	3.06	405	0.061	-16.54	179a	189a	0.5151	0.109	0.587	0.062	HOMO	LUMO+9
									178a	188a	0.2613	-0.404	0.106	-0.146	HOMO–1	LUMO+8
									179a	188a	0.0404	-0.339	0.118	0.085	HOMO	LUMO+8
				27	3.08	403	0.118	28.69	178a	188a	0.3895	-0.492	0.129	-0.178	HOMO–1	LUMO+8
									179a	189a	0.3788	-0.093	-0.502	-0.053	HOMO	LUMO+9
									179a	188a	0.032	-0.301	0.105	0.075	HOMO	LUMO+8
				29	3.13	396	0.072	-5.50	177a	188a	0.7184	0.021	-0.441	-0.797	HOMO–2	LUMO+8
									178a	189a	0.1116	-0.193	0.188	-0.162	HOMO–1	LUMO+9
									175a	180a	0.0239	-0.036	-0.012	-0.037	HOMO–4	LUMO
V	369s	5	369	40	3.26	380	0.054	13.43	177a	189a	0.5833	0.095	-0.879	-0.101	HOMO–2	LUMO+9
				42	3.29	377	0.057	-30.96	175a	182a	0.532	-0.451	0.031	-0.104	HOMO–4	LUMO+2
									172a	180a	0.164	-0.535	0.263	-0.168	HOMO–7	LUMO
				44	3.31	374	0.063	22.17	174a	182a	0.7734	-0.192	-0.587	0.382	HOMO–5	LUMO+2
									172a	180a	0.0429	0.273	-0.134	0.086	HOMO–7	LUMO
				49	3.36	369	0.082	39.46	179a	192a	0.5011	0.568	0.381	-0.246	HOMO	LUMO+12
				56	3.42	362	0.052	-63.64	171a	180a	0.495	0.311	0.052	-0.225	HOMO–8	LUMO
									177a	190a	0.1335	0.048	-0.095	0.291	HOMO–2	LUMO+10
									172a	182a	0.1223	0.272	0.029	-0.590	HOMO–7	LUMO+2
				57	3.43	361	0.055	9.13	177a	190a	0.3231	0.075	-0.148	0.453	HOMO–2	LUMO+10
									178a	192a	0.2266	-0.040	0.213	-0.240	HOMO–1	LUMO+12
									172a	182a	0.1207	-0.269	-0.029	0.585	HOMO–7	LUMO+2
				59	3.45	360	0.059	-4.65	175a	184a	0.4575	-0.230	0.181	0.231	HOMO–4	LUMO+4
									178a	192a	0.1695	0.034	-0.184	0.207	HOMO–1	LUMO+12
									177a	190a	0.1176	0.045	-0.089	0.272	HOMO–2	LUMO+10

									172a	182a	0.0621	-0.193	-0.021	0.418	HOMO–7	LUMO+2
				64	3.50	355	0.074	87.85	171a	181a	0.3819	0.506	0.306	-0.329	HOMO–8	LUMO+1
									172a	183a	0.1505	0.049	0.127	0.050	HOMO–7	LUMO+3
									170a	180a	0.1423	0.127	-0.308	0.324	HOMO–9	LUMO
				67	3.54	351	0.088	49.23	170a	180a	0.3136	-0.188	0.454	-0.478	HOMO–9	LUMO
									177a	192a	0.0942	0.023	0.161	0.005	HOMO–2	LUMO+12
									172a	184a	0.0527	-0.152	0.052	0.028	HOMO–7	LUMO+4
Vi	330s	6	333													
				69	3.56	348	0.094	-172.14	169a	180a	0.575	0.206	0.004	-0.461	HOMO–10	LUMO
									170a	180a	0.0955	-0.103	0.250	-0.263	HOMO–9	LUMO
				75	3.63	342	0.051	51.12	169a	181a	0.6681	-0.733	-0.570	0.264	HOMO–10	LUMO+1
				76	3.64	341	0.009	-7.78	168a	180a	0.7958	-0.205	0.057	-0.143	HOMO–11	LUMO
									169a	181a	0.0543	0.209	0.162	-0.075	HOMO–10	LUMO+1
				80	3.68	337	0.037	6.47	172a	185a	0.5891	0.162	-0.313	0.328	HOMO–7	LUMO+5
									170a	182a	0.1637	0.089	-0.344	0.127	HOMO–9	LUMO+2
				81	3.69	336	0.047	54.55	169a	182a	0.7974	-0.672	0.339	-0.469	HOMO–10	LUMO+2
				83	3.72	334	0.049	-17.41	171a	184a	0.4048	0.168	0.470	0.322	HOMO–8	LUMO+4
									167a	180a	0.21	0.133	0.271	0.447	HOMO–12	LUMO
				85	3.73	333	0.064	-66.01	168a	181a	0.3774	0.415	-0.471	0.197	HOMO–11	LUMO+1
									176a	187a	0.1951	0.170	-0.085	0.012	HOMO–3	LUMO+7
									167a	180a	0.1755	0.121	0.247	0.408	HOMO–12	LUMO
				89	3.76	330	0.166	55.86	179a	193a	0.6479	-1.089	0.019	0.685	HOMO	LUMO+13
				93	3.79	327	0.047	-5.28	168a	182a	0.5068	0.101	-0.054	-0.671	HOMO–11	LUMO+2
									174a	187a	0.2187	0.196	-0.039	-0.058	HOMO–5	LUMO+7
				97	3.83	324	0.050	-4.39	170a	184a	0.4232	-0.452	-0.453	-0.099	HOMO–9	LUMO+4
									169a	183a	0.3176	-0.396	0.445	0.082	HOMO–10	LUMO+3
									178a	193a	0.0743	-0.031	0.329	0.050	HOMO–1	LUMO+13
				101	3.86	322	0.094	-4.04	171a	185a	0.2443	0.177	0.276	0.289	HOMO–8	LUMO+5
									169a	184a	0.2338	-0.250	-0.210	0.008	HOMO–10	LUMO+4
									172a	186a	0.1232	0.096	0.123	0.293	HOMO–7	LUMO+6
				102	3.86	321	0.061	125.60	168a	183a	0.2997	-0.104	0.333	-0.073	HOMO–11	LUMO+3
									167a	182a	0.2249	0.017	0.278	0.284	HOMO–12	LUMO+2
									178a	193a	0.1048	-0.036	0.390	0.059	HOMO–1	LUMO+13
				103	3.87	320	0.060	-49.91	169a	184a	0.4856	0.359	0.302	-0.012	HOMO–10	LUMO+4
									170a	184a	0.1377	0.257	0.257	0.056	HOMO–9	LUMO+4
									168a	183a	0.1193	0.065	-0.210	0.046	HOMO–11	LUMO+3
				105	3.89	319	0.079	11.42	172a	187a	0.5797	0.712	-0.374	0.115	HOMO–7	LUMO+7
				112	3.95	314	0.084	-36.56	170a	185a	0.3151	-0.127	-0.382	-0.254	HOMO–9	LUMO+5
									167a	183a	0.1489	-0.191	0.037	-0.133	HOMO–12	LUMO+3
									168a	184a	0.1073	-0.104	0.162	-0.245	HOMO–11	LUMO+4
									177a	193a	0.0858	-0.128	0.035	-0.165	HOMO–2	LUMO+13
				113	3.96	314	0.110	-50.47	179a	195a	0.4252	0.754	-0.112	-0.356	HOMO	LUMO+15

				114	3.96	313	0.081	20.98	168a	184a	0.4451	-0.211	0.330	-0.499	HOMO–11	LUMO+4
									179a	195a	0.1343	0.424	-0.063	-0.200	HOMO	LUMO+15

Table S7. Optical absorption and CD data for $[Au_8(L1)_3(PH_3)]^{2+}$ (8): peak positions, excited state wavelength, oscillator strengths (*f*), rotatory strengths (*R*, 10^{-40} esu^{2}cm^2), and orbitals involved in electronic transitions. Method LB94/DZ.fc (in chloroform).

				Excited state			f	R				Transition dipole moment				
ABS		CD							Electron transitions		Weight				Orbitals involved	
#	Peak nm	#	Peak nm	no.	E/eV	E/nm			From	To		x	y	z	from	to
I	530	1	548	2B	2.26	548	0.030	157.52	71a	70b	0.621	-2.034	-1.763	0.000	HOMO–1	LUMO+1
									69b	72a	0.240	-1.544	-0.528	0.000	HOMO	LUMO
									69b	73a	0.107	1.120	0.673	0.000	HOMO	LUMO+3
				3B	2.32	534	0.272	15.91	71a	71b	0.980	0.360	0.177	0.000	HOMO–1	LUMO+2
									71a	70b	0.008	0.217	0.188	0.000	HOMO–1	LUMO+1
									69b	73a	0.005	-0.231	-0.139	0.000	HOMO	LUMO+3
				4A	2.34	529	0.330	-13.05	71a	73a	0.815	0.000	0.000	-3.114	HOMO–1	LUMO+3
									68b	70b	0.066	0.000	0.000	0.733	HOMO–2	LUMO+1
									71a	72a	0.043	0.000	0.000	-0.639	HOMO–1	LUMO
									69b	70b	0.040	0.000	0.000	-0.601	HOMO	LUMO+1
		2	495	5A	2.49	498	0.002	-8.88	69b	72b	0.749	0.000	0.000	-0.376	HOMO	LUMO+4
				6B	2.51	494	0.012	-21.06	71a	72b	0.502	0.262	-0.993	0.000	HOMO–1	LUMO+4
									69b	74a	0.465	0.976	-0.555	0.000	HOMO	LUMO+5
II	425	3	420	7B	2.91	426	0.633	-104.34	69b	75a	0.950	1.015	0.691	0.000	HOMO	LUMO+6
				8A	2.92	424	0.634	-110.88	68b	70b	0.851	0.000	0.000	-2.406	HOMO–2	LUMO+1
				9A	3.04	408	0.020	-16.61	68b	71b	0.974	0.000	0.000	0.177	HOMO–2	LUMO+2
				10A	3.09	401	0.014	-41.84	70a	72a	0.900	0.000	0.000	-0.494	HOMO–3	LUMO
				11B	3.10	400	0.083	-106.80	66b	72a	0.886	-0.362	-0.087	0.000	HOMO–6	LUMO
				12B	3.21	386	0.092	84.66	67b	72a	0.399	-0.048	0.219	0.000	HOMO–5	LUMO
									71a	73b	0.206	0.228	0.146	0.000	HOMO–1	LUMO+7
III	353	4	352	13B	3.30	376	0.041	14.75	69b	76a	0.832	0.022	0.174	0.000	HOMO	LUMO+8
				14A	3.32	374	0.040	10.80	71a	76a	0.345	0.000	0.000	-0.327	HOMO–1	LUMO+8
				15B	3.51	353	0.873	-110.00	69b	77a	0.975	0.719	0.354	0.000	HOMO	LUMO+10
				16A	3.51	353	0.889	-133.54	69b	73b	0.516	0.000	0.000	-0.244	HOMO	LUMO+7
				17A	3.73	332	0.008	-1.55	71a	77a	0.698	0.000	0.000	0.464	HOMO–1	LUMO+10
				18A	3.82	325	0.022	5.89	69b	75b	0.746	0.000	0.000	-0.266	HOMO	LUMO+11
				19B	3.82	324	0.022	4.30	71a	75b	0.840	-0.243	-0.104	0.000	HOMO–1	LUMO+11

Table S8. Optical absorption and CD data for $[Au_8(L2)_3(PH_3)]^{2+}$ (9): peak positions, excited state wavelength, oscillator strengths (*f*), rotatory strengths (*R*, 10^{-40} esu^2cm^2), and orbitals involved in electronic transitions. Method LB94/DZ.fc (in chloroform).

				Excited state								Transition dipole moment				
ABS		CD					f	R	Electron transitions		Weight				Orbitals involved	
#	Peak, nm	#	Peak, nm	no.	E/eV	E/nm			From	To		x	y	z	from	to
I	565	1	587	2B	2.12	585	0.0214	202.58	68a	67b	0.625	2.126	1.740	0.000	HOMO–1	LUMO+1
									66b	69a	0.239	1.550	0.562	0.000	HOMO	LUMO
									66b	70a	0.108	-1.105	-0.637	0.000	HOMO	LUMO+2
				3B	2.19	566	0.2496	-33.577	68a	68b	0.958	0.366	0.300	0.000	HOMO–1	LUMO+3
									66b	70a	0.022	-0.467	-0.269	0.000	HOMO	LUMO+2
		2	553	4A	2.20	564	0.2860	-54.298	68a	70a	0.729	0.000	0.000	3.001	HOMO–1	LUMO+2
II	474	3	470	7B	2.58	480	0.4588	-139.86	68a	70b	0.705	0.591	0.911	0.000	HOMO–1	LUMO+5
									66b	71a	0.141	0.460	0.023	0.000	HOMO	LUMO+6
									66b	70a	0.035	0.559	0.322	0.000	HOMO	LUMO+2
				8A	2.60	477	0.3607	-85.414	68a	71a	0.031	0.000	0.000	0.176	HOMO–1	LUMO+6
									66b	67b	0.003	0.000	0.000	0.147	HOMO	LUMO+1
				9A	2.67	465	0.2117	-117.98	68a	72a	0.945	0.000	0.000	-0.172	HOMO–1	LUMO+8
									68a	73a	0.020	0.000	0.000	-0.083	HOMO–1	LUMO+9
									66b	70b	0.012	0.000	0.000	0.106	HOMO	LUMO+5
				10B	2.68	462	0.1132	-68.715	66b	73a	0.849	-0.485	-0.346	0.000	HOMO	LUMO+9
									65b	69a	0.064	0.595	0.335	0.000	HOMO–2	LUMO
III	450	3		11A	2.77	448	0.0974	-18.493	68a	71a	0.001	0.000	0.000	0.032	HOMO–1	LUMO+6
									66b	72b	0.799	0.000	0.000	-0.022	HOMO	LUMO+10
									68a	74a	0.192	0.000	0.000	0.024	HOMO–1	LUMO+11
									68a	73a	0.002	0.000	0.000	-0.028	HOMO–1	LUMO+9
									66b	70b	0.001	0.000	0.000	-0.027	HOMO	LUMO+5
				12B	2.78	447	0.0384	-24.879	65b	69a	0.851	2.118	1.193	0.000	HOMO–2	LUMO
				13B	2.80	443	0.2537	-75.669	68a	72b	0.567	-0.487	0.873	0.000	HOMO–1	LUMO+10
									66b	74a	0.392	-0.507	0.679	0.000	HOMO	LUMO+11
									67a	68b	0.010	0.175	-0.310	0.000	HOMO–3	LUMO+3
				14A	2.81	442	0.1905	-39.906	68a	75a	0.805	0.000	0.000	1.503	HOMO–1	LUMO+12
				17B	3.01	412	0.0000	-3.5551	65b	70a	0.874	0.151	-0.246	0.000	HOMO–2	LUMO+2
IV	371	4	372	22B	3.26	380	0.0016	-11.025	66a	68b	0.877	-0.498	-0.045	0.000	HOMO–4	LUMO+3
									65b	72a	0.086	0.270	0.147	0.000	HOMO–2	LUMO+8
				23A	3.27	379	0.0050	-24.407	67a	70a	0.829	0.000	0.000	-0.097	HOMO–3	LUMO+2
									64b	68b	0.055	0.000	0.000	-0.070	HOMO–5	LUMO+3
									66b	74b	0.024	0.000	0.000	0.094	HOMO	LUMO+15
									65b	71b	0.009	0.000	0.000	0.105	HOMO–2	LUMO+7
									65a	70a	0.004	0.000	0.000	-0.001	HOMO–7	LUMO+2
				24B	3.32	373	0.4640	-227.2	66b	76a	0.923	-0.156	-0.243	0.000	HOMO	LUMO+14

				25A	3.33	373	0.4743	-195.6	64b	68b	0.693	0.000	0.000	-0.248	HOMO–5	LUMO+3
									66a	70a	0.189	0.000	0.000	0.668	HOMO–4	LUMO+2
V	346	4		26B	3.36	369	0.0741	104.65	67a	69b	0.489	0.459	-0.836	0.000	HOMO–3	LUMO+4
									67a	68b	0.431	-1.034	1.838	0.000	HOMO–3	LUMO+3
				27B	3.57	348	0.3472	-90.145	68a	74b	0.327	0.110	-0.011	0.000	HOMO–1	LUMO+15
									68a	73b	0.274	-0.405	-0.297	0.000	HOMO–1	LUMO+13
									65b	72a	0.247	0.454	0.247	0.000	HOMO–2	LUMO+8
				28A	3.58	346	0.2715	-53.001	66b	74b	0.449	0.000	0.000	0.403	HOMO	LUMO+15
									68a	77a	0.380	0.000	0.000	-0.131	HOMO–1	LUMO+16
									68a	76a	0.105	0.000	0.000	-0.204	HOMO–1	LUMO+14
				29A	3.65	340	0.1603	-10.178	66b	73b	0.599	0.000	0.000	0.474	HOMO	LUMO+13
									66a	70a	0.104	0.000	0.000	0.490	HOMO–4	LUMO+2
									65a	69a	0.046	0.000	0.000	0.298	HOMO–7	LUMO
				30B	3.65	339	0.1404	0.21868	68a	73b	0.466	-0.524	-0.384	0.000	HOMO–1	LUMO+13
				31B	3.69	336	0.0006	-30.346	66a	69b	0.767	-0.502	-0.196	0.000	HOMO–4	LUMO+4
				33B	3.71	334	0.0065	72.485	62b	69a	0.439	0.306	0.226	0.000	HOMO–9	LUMO
									64a	67b	0.382	-0.312	-0.146	0.000	HOMO–8	LUMO+1
				35B	3.74	332	0.0116	-14.233	66b	78a	0.804	0.168	-0.004	0.000	HOMO	LUMO+17

References

1. Takano, S.; Tsukuda, T., Amplification of the Optical Activity of Gold Clusters by the Proximity of BINAP. *J. Phys. Chem. Lett.* **2016,** *7*, 4509-4513.
2. McKenzie, L. C.; Zaikova, T. O.; Hutchison, J. E., Structurally Similar Triphenylphosphine-Stabilized Undecagolds, $Au_{11}(PPh_3)_7Cl_3$ and $Au_{11}(PPh_3)_8Cl_2Cl$, Exhibit Distinct Ligand Exchange Pathways with Glutathione. *J. Am. Chem. Soc.* **2014,** *136*, 13426-13435.
3. Provorse, M. R.; Aikens, C. M., Origin of Intense Chiroptical Effects in Undecagold Subnanometer Particles. *J. Am. Chem. Soc.* **2010,** *132*, 1302-1310.